Zhengfang Li
Zhengyuan Gao ✉
Zhiguo An
Yanping Sun
Bin Wu
Youwen Zhai

https://doi.org/10.21278/TOF.474053423
ISSN 1333-1124
eISSN 1849-1391

A NOVEL TEMPERATURE MODEL OF REGIONS FORMED DURING THE PREHEATING STAGE OF BELT HEATING IN INCREMENTAL SHEET FORMING

Summary

The temperature of a forming region has a gradient distribution characteristic in the belt heating incremental sheet forming process, in which the relation between the heating power and the temperature distribution is ambiguous in the pre-heating stage. The setup of the heating power is therefore challenging, and the whole forming efficiency might decrease due to the above issue. Therefore, this paper proposes a belt heating method for electric conduction heating and presents a temperature calculation model for the forming region of the plate in the preheating state based on the heat conduction model. The calculated accuracy of the model is analysed through physical experiments, and the thermal transfer efficiency of heating tubes is analysed in detail. Based on the result, the thermal transfer efficiency value for heating tubes is determined to improve the accuracy of the suggested model. In addition, the effect of the model slope on the calculated result is further analysed, and the setting method of the slope value for the model is proposed according to different accuracy requirements.

Key words: *incremental sheet forming, temperature model, hot forming, pre-heating process, belt heating*

1. Introduction

Incremental Sheet Forming (ISF), which combines rapid prototyping with plastic forming, is a flexible dieless forming technology [1-2]. This technology can effectively reduce some production indicators, such as the manufacturing cycle and energy consumption. Meanwhile, the formability limit of materials is also significantly improved. Therefore, this technology has a wide range of potential applications for aerospace, transportation, energy equipment, and medical and other fields.

With the rapid development of industry, lightweight alloys have been gradually applied to various products, especially in the automotive, aerospace, and defence industries [3-5]. Meanwhile, the application of aluminium alloys is most widespread in the application of light

alloys. High-strength aluminium alloys have poor formability at room temperature but they have fine formability at elevated temperatures. As a result, the complex part is fabricated with difficulty through the traditional incremental sheet forming process [6-9]. In order to fabricate parts with high-strength aluminium alloys, the hot incremental sheet forming process is proposed to fabricate complex parts with high-strength aluminium alloys [10-13]. In recent years, various heat methods (as shown in Fig.1 [14-19]), such as laser heat [14], thermal medium heat [15-16], electrically assisted heat [17-18], and electromagnetic induction heat [19], have been proposed to rapidly increase the deformation temperature during the forming process, and then the part with high-strength aluminium alloys can be successfully fabricated through the hot incremental sheet forming process. Laser heat and electromagnetic induction heat have a wide heating range, which can fabricate the various lightweight alloy part. However, the two methods can lead to higher equipment maintenance costs, and the fabricated cost of the part is also increased. Meanwhile, a hot medium system and a heat-insulation device need to be set in thermal medium heat, and the heat efficiency of the method is lower than the first two methods. Compared to the aforementioned method, electrically assisted heat has many advantages, such as high heat efficiency, a simple device, low cost, and a simple structure. Therefore, electrically assisted heat is widely used in the hot incremental forming of high-strength aluminium alloys due to the fact that the hot method has high heat efficiency and a simple device structure [20-23]. In electrically assisted heat, two types, such as self-resistance heat and thermal conduction heat, are usually adopted to fabricate the part with high-strength aluminium alloys. The thermal conduction heat method is more reliable due to the fact that the self-resistance heating method has the defect of arcing burn [24].

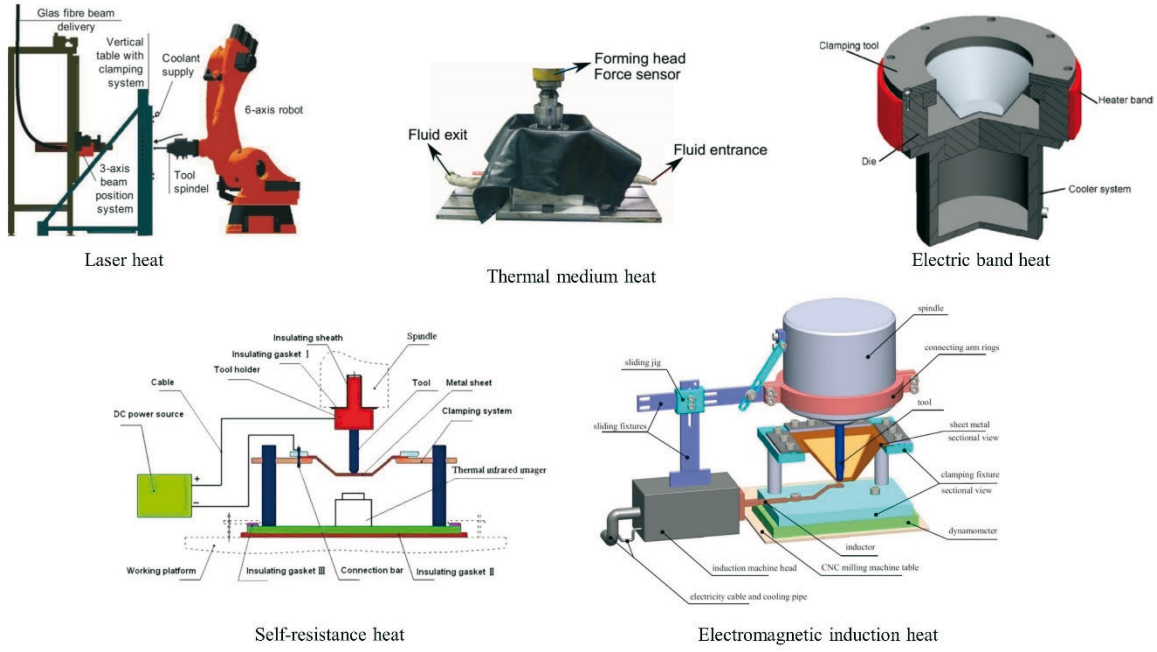

Fig. 1 Sketch of different heat methods

According to the above analysis, the thermal conduction heat device has a closed structure, which leads to a narrow processing range for hot incremental sheet forming. In order to solve this issue, the paper proposes a belt heating method (as shown in Fig. 2) and presents a temperature calculation model for the forming region of the plate in the preheating state based on the heating method. The thermal transfer efficiency, which is determined through physical experiments, of heating tubes on the calculated accuracy is analysed in detail. In addition, the set method of slope value for the model is proposed according to different accuracy requirements.

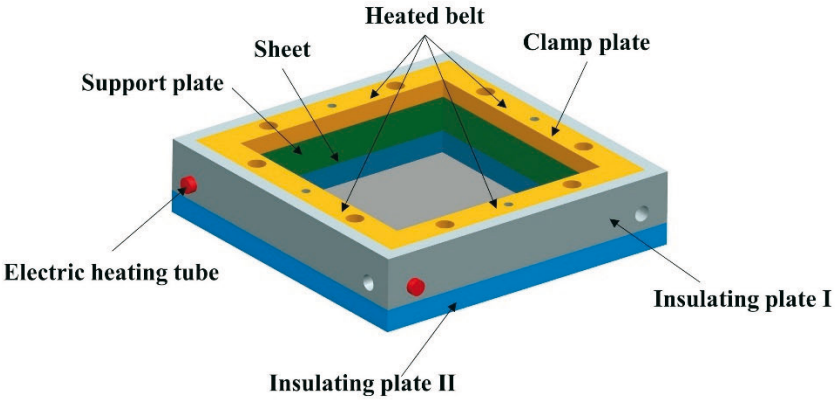

Fig. 2 Sketch of the belt heating method

2. Materials and models

In this section, some research foundations, such as materials, experimental setups, preheating temperature characteristics, and temperature models for the forming region, are introduced in detail. In subsequent sections, the models established are verified based on the method of combining the numerical simulation with experiments.

2.1 Materials and setups

The square plate with AA2024-T4 aluminium is adopted to analyse the static saturation temperature of the forming region. The thickness of the plate is 1mm, and the side length is 200mm. As shown in Fig. 2, the hot-working die steel of H13, which has good strength at high temperatures, is used to fabricate the clamp plate and the support plate, and the mica is adopted to fabricate insulating plates. The use of insulating plates can limit the heat loss at the edge.

Fig. 3 shows the heating system of the forming device in which the power regulator is used to control the power of each heating tube. Meanwhile, K-type temperature sensors (range: 0-1300 °C) are used to obtain temperature signals of the forming region and the clamp region, and the multichannel temperature collector is adopted to obtain the temperature value of the two regions.

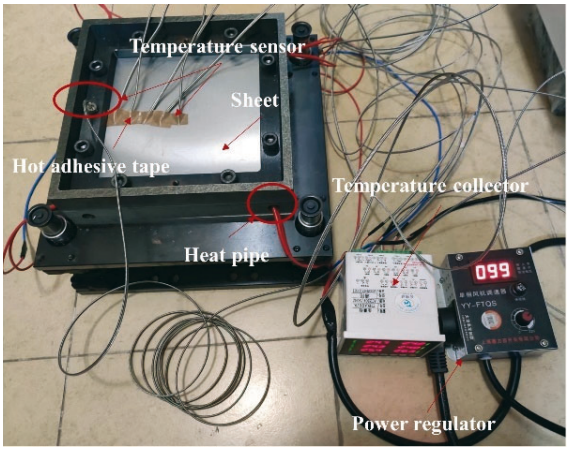

Fig. 3 Sketch of the heating system of the forming device

2.2 Distribution characteristics of the preheating temperature

Fig. 4 shows the transfer process of the thermal flow in the belt heating method, and the numerical simulation of the preheating process is used to preliminarily estimate the temperature distribution characteristics of the forming region. Four heating tubes are used to increase the temperature of the support plate and the region, which is the contact area between the clamp plate and the sheet. Accordingly, the forming region obtains thermal energy through the heat transfer of the support plate. The region between the sheet, the clamp, and the air will produce a heat loss due to the heat convection of air. The temperature of the forming region is gradually increased through the internal heat transfer of the sheet.

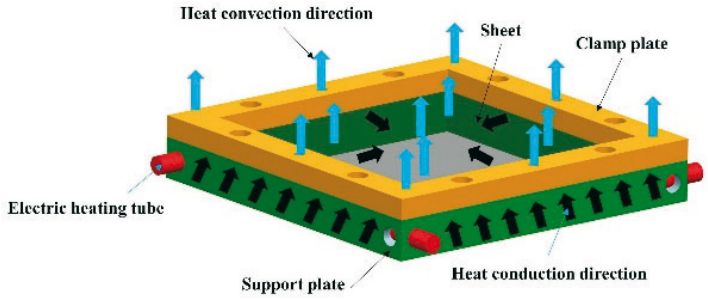

Fig. 4 Thermal transfer of the heating system

Fig. 5 shows the finite element model of the preheating process, and the module of the heat transfer of the finite element software is adopted to analyse the temperature characteristics of the forming region in the preheating stage. The element of the support plate and the clamp plate is a 10-node element of DC3D10, and the element of DS4 is adopted to mesh the heating tubes. The 8-node element of DC3D8 is used to analyse the preheating temperature of the sheet.

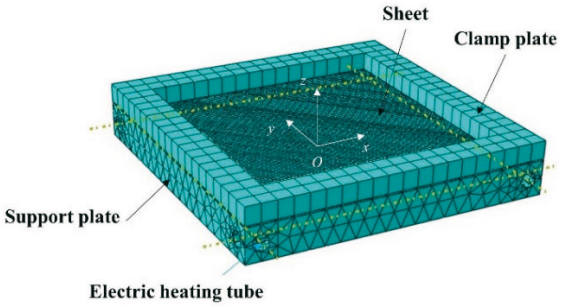

Fig. 5 Finite element model of the heating system

Table 1 shows the major heat parameters, namely those that are obtained through the thermal experiments, in the preheating stage simulation, in which the other components include the clamp plate, the support plate, and the heat convection. The heat convection is mainly that between the sheet and the air, and the corresponding heat parameters are separately the heat convection of the air and the sinking temperature.

A surface heat flux is set to provide initial heat for the heating system, and a surface heat flux of 0.018 W/mm^2, which is equal to 100 W power of each heating tube, is set to analyse the temperature characteristics of the forming region in the preheating stage. Fig. 6 shows the result of the simulation based on the above setup, and the temperature of the forming region has the characteristic of symmetrical distribution. Meanwhile, the edge of the forming region has a max temperature, and the temperature of the forming region gradually decreases from the edge to the centre. Therefore, the temperature of the forming region has the characteristic of the symmetrical distribution of the temperature gradient.

Table 1 Simulation parameters of the preheating stage

Category	Sheet	Tube	Other components
Conductivity, W/mm°C	0.234	0.02	0.032
Specific heat, J/kg°C	900	500	460
Density, kg/mm^3	2.7×10^{-6}	8×10^{-6}	7.8×10^{-6}
Heat convection of air, W/mm^2°C	-	-	2.5×10^{-5}
Sinking temperature, °C	-	-	10

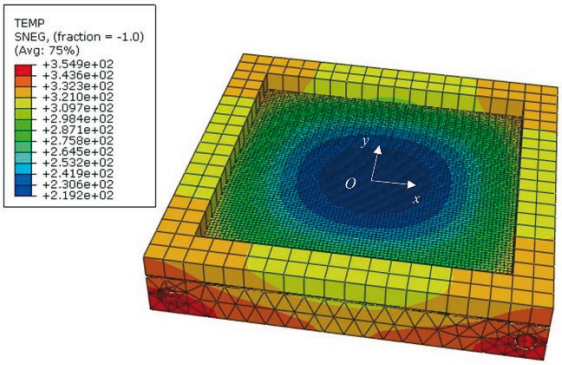

Fig. 6 Results of the numerical simulation

2.3 Temperature models of the forming region

The temperature distribution of the sheet metal forming region has an axisymmetric characteristic according to the result from Fig. 6. The temperature distribution of the region also has the characteristic of a contour line. Therefore, the temperature change along the *x*-axis is consistent with that along the *y*-axis, and then the temperature distribution of the sheet metal forming region is simplified as the heat conduction characteristic of a rod. Therefore, the unit body (Fig. 7), which includes the support plate, the clamp plate, and the sheet, is adopted to describe the temperature of the forming region. The thermal energy of the heating tubes transfers to the support plate, and Q1 is used to describe the thermal energy of the unit of the support plate. Q2 is the thermal energy of the region, which is between the support plate and the clamp plate in Fig. 6. Q4 is the thermal energy of the unit of the forming region.

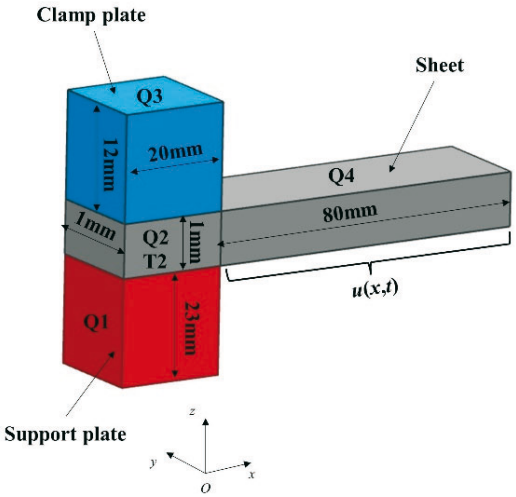

Fig. 7 Sketch of the unit body

It is assumed that the thermal energy of the heating tubes is transferred to the support plate in the form of volume density. Therefore, Q of the unit body is obtained:

$$Q=\eta \frac{Plh}{V} t, \tag{1}$$

where Q is the total thermal energy of the unit body, η is the thermal transfer efficiency of the heating pipes, P is the power of the heating pipes, and V is the volume of the support plate. l and h are the length and the height of the support unit, respectively, and t is the heating time.

According to Fig. 5, the temperature distribution of the forming region is relatively uniform in the width and thickness directions, and the thermal transfer of the forming region is only considered to vary in the length direction. In this paper, the length direction is assumed to be the x-axis. Therefore, the thermal energy of the unit of the forming region is written as Eq. (2) according to the law of conservation of heat:

$$Q_{in}=Q_T + Q_{out}, \tag{2}$$

where Q_{in} is the absorbed heat of the unit of the forming region, Q_T is the total heat of the unit, and Q_{out} is the loss of heat of the unit. Therefore, Q_{in} is further written as follows:

$$Q_{in}=\int_{t_1}^{t_2}\int_{x_1}^{x_2} c_1\rho \frac{\partial u}{\partial t}\mathrm{d}x\mathrm{d}t, \tag{3}$$

where u (x, t) is the temperature function of the unit of the forming region, and c_1 is the specific heat of the sheet, and ρ is the density of the sheet.

The width and the height of the forming unit are constant, and the temperature of directions is uniform. Therefore, the total heat of the forming unit can be written as follows:

$$Q_T=\int_{t_1}^{t_2}\int_{x_1}^{x_2} k_1 \frac{\partial u}{\partial x}\mathrm{d}x\mathrm{d}t, \tag{4}$$

where k_1 is the thermal conductivity of the sheet. Meanwhile, the lost heat (Eq. (5)) of the forming unit is further obtained according to the thermal convection phenomenon in the following form:

$$Q_{out}=2k_2\int_{t_1}^{t_2}\int_{x_1}^{x_2}(u-u_1)\,\mathrm{d}x\mathrm{d}t, \tag{5}$$

where u_1 is the temperature of the air and is equal to the room temperature, and k_2 is the surface thermal conductivity between the sheet and air. Therefore, Eq. (2) is further written as follows:

$$\int_{t_1}^{t_2}\int_{x_1}^{x_2} c_1\rho \frac{\partial u}{\partial t}\mathrm{d}x\mathrm{d}t = \int_{t_1}^{t_2}\int_{x_1}^{x_2} k_1 \frac{\partial u}{\partial x}\mathrm{d}x\mathrm{d}t + 2k_2\int_{t_1}^{t_2}\int_{x_1}^{x_2}(u-u_1)\,\mathrm{d}x\mathrm{d}t. \tag{6}$$

It is assumed that t_1 is 0, and x_1 is the edge of the forming unit and is also viewed as 0. Meanwhile, x_2 is the distance from the edge to the centre of the forming unit. Consequently, Eq. (6) can be written as follows:

$$\int_{t_1}^{t_2}\int_{x_1}^{x_2}[c_1\rho u_t - k_1 u_x - 2k_2(u-u_1)]\,\mathrm{d}x\mathrm{d}t = 0. \tag{7}$$

According to Eq. (7), two sides of the equation are both divided by $c_1\rho$, and α is equal to $k_1/c_1\rho$, and λ is equal to $2k_2/c_1\rho$. Therefore, Eq. (7) is further written as follows:

$$u_t - \alpha u_x - \lambda(u-u_1) = 0. \tag{8}$$

As shown in Fig. 7, the forming unit is viewed as the heat transfer of a rod. Therefore, if t is constant, the temperature of the forming unit should be written as follows:

$$T(x) = C_1 x + C_2. \tag{9}$$

Since the room temperature is u_1, the initial temperature of the forming unit is also u_1. Therefore, u is equal to u_1 when t is equal to 0, and $u_t|_{x=0}$ is equal to T_2 (the edge temperature of the sheet unit), and $u_x|_{t=0}$ is equal to 0. The initial condition of the forming unit is written as follows:

$$u|_{x=0} = T_2. \tag{10}$$

Combining Eqs. (9)-(10), C_2 is equal to T_2. Combining the simulation result, T_2 can be written as follows:

$$T_2 = 3.37P^{0.98}e^{-7.118\times10^{-7}t} - 3.25P^{0.99}e^{-0.00079t}. \tag{11}$$

According to the above analysis, Eq. (9) is further written as follows:

$$u(x,t) = C_1 x + T_2(t). \tag{12}$$

Meanwhile, u (x, t) is equal to T (x, t) when t is constant. Combining Eqs. (8), C_1 is obtained:

$$C_1 = \frac{T_2'(t)+\lambda u_1-\lambda T_2(t)}{\lambda x+\alpha}, \tag{13}$$

where T_2'(t) is written as follows:

$$T_2'(t) = 2.57\times10^{-3}P^{0.99}e^{-0.00079t} - 23.99\times10^{-7}P^{0.98}e^{-7.118\times10^{-7}t}. \tag{14}$$

3. Results and discussion

3.1 Analysis of the temperature model

It is assumed that the thermal transfer efficiency is 100%, namely that η is 1. k_2 is approximately 0.0005 W/mm^2 based on the experimental result. The temperature model proposed is used to calculate the temperature of the forming unit, and the space of the x direction is 20 mm.

The power values, such as 50-, 100-, and 200-W, are set to analyse the static saturation temperature of the forming unit. Fig. 8 shows the difference between the simulation value, the calculated value, and the actual value. The temperature of the forming unit is gradually reduced from the edge to the centre, and the change is approximate to a linear decreasing trend. The max error of each power is both less than 10%, and then the accuracy of the temperature model proposed is validated. Therefore, the temperature model can accurately describe the change trend of the static saturation temperature for the forming region.

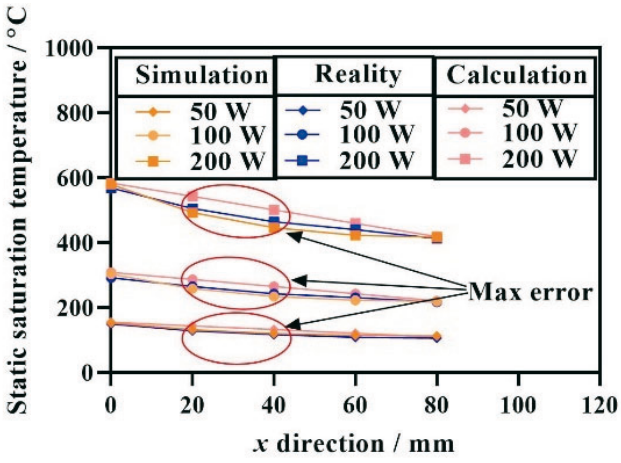

Fig. 8 Static saturation temperature for different power

3.2 Assigned η for the temperature model

According to the previous analysis, the value of η is assumed as 1, and the calculation result of the model is consistent with the actual value. However, there is a difference between the calculation and reality, and so the thermal loss of the heating tubes should be considered to improve the accuracy of the model.

Fig. 9 shows the effect of η on the static saturation temperature when x is 0 mm. The static saturation temperature of each power gradually decreases with the decrease of η, and the amplitude of the decrease is significant. Therefore, the effect of η on the static saturation temperature is significant in the belt heating method. The difference between the actual value and the calculation value (η=1) is 5.2 °C when the power is 50 W, and the difference of 100 W is 13 °C, and that of 200 W is 31.9 °C. According to the above analysis, the error percentage is 3.5%, 4.5%, and 5.6% respectively, and the average error percentage is 4.5%. Therefore, η is set as 95.5% in the belt heating method according to the previous analysis.

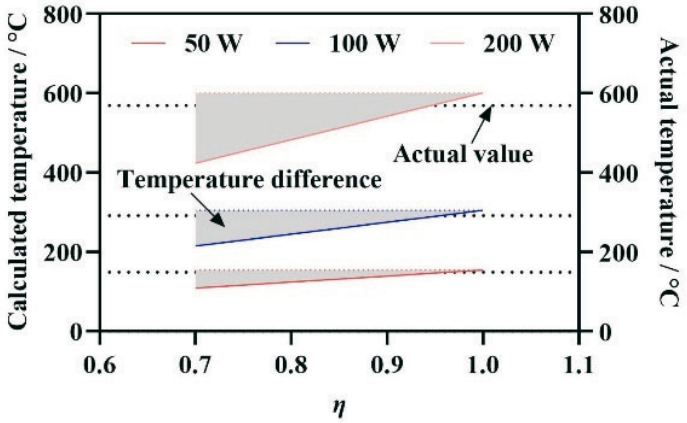

Fig. 9 Effect of η on the static saturation temperature

Fig. 10 shows the calculated result of the x direction under the action of 0.955 η. The static saturation temperature of 0- and 80- x approaches the actual value, and the max difference between the calculated value and the actual value is mainly located in the range of 20- to 40- x. Although the difference between the calculated model and the actual result still exists under the action of 0.955 η, the calculated accuracy of the model is improved compared to the case where η is set as 1.

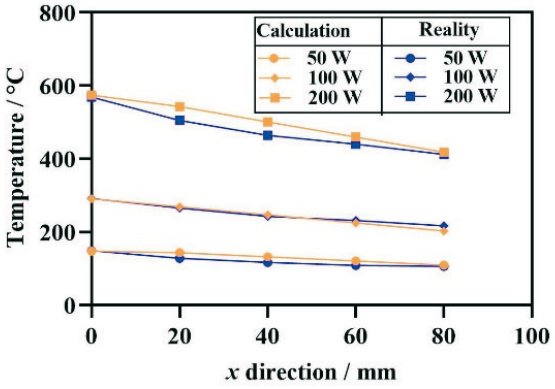

Fig. 10 Analysis of the calculated result of 0.955 η

3.3 Effect of the model slope on the temperature calculated

According to the above analysis, C_1 is a significant factor for the temperature gradient of the forming region when t is determined, and the value of C_1 changes with x. Fig. 11 shows the change trend of C_1 changing with x under the action of different powers. The value of C_1 is

positively correlated with the power, namely that C_1 has an approximately equal proportion change with the power. In addition, the absolute value of C_1 changes from large to small with the increase of x, and the curve slope of C_1 has a certain degree of reduction when the value of x is greater than 40 mm, and then the temperature change amplitude of the forming region is gentle when x is greater than or equal to 40. Meanwhile, C_1 of each power fluctuates around the corresponding mean value. Therefore, the mean value of C_1 can be adopted to calculate the temperature gradient of the forming region, which needs to be further analysed.

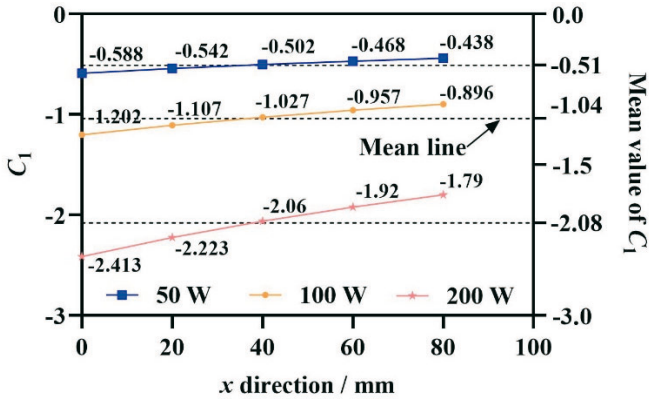

Fig. 11 The changing trend of C_1 with the increase of x

Fig. 12 shows the temperature error under the action of the mean value of C_1. The error of 5% is used to estimate the calculated accuracy of the model under the action of the mean value of C_1, in which the actual result is viewed as A_1. The calculated result with C_1 is represented by A_2, and the calculated result with the mean value of C_1 is viewed as A_3. The difference, namely that the collection point is respectively the position of 20- and 40- mm under the action of 50- and 200- W, between A_1 and A_3, is greater than 5%. The difference is both less than 5% under the action of 100 W, and the error between A_1 and A_2 is both less than 5% for each power. The error, namely the position of 20- and 40- mm, between A_1 and A_3 is respectively 9.58 mm and 10.95 mm under the action of 100 W, and the corresponding error for 200 W is respectively 27.65 mm and 26.89 mm. The former error percentage is respectively 7.1% and 8.8%, and the latter is 5.5% and 5.8%. According to the above analysis, the error percentage between A_1 and A_3 is in the range of 0 to 10% under the action of each power, and then the mean value of C_1 is used to ensure the calculated accuracy of 10% of the model proposed. Therefore, if the calculated accuracy of the model is higher, the calculated value of C_1 should be calculated to obtain the temperature gradient of the forming region. On the other hand, the mean value of C_1 can be used to simplify the calculated model of the temperature gradient.

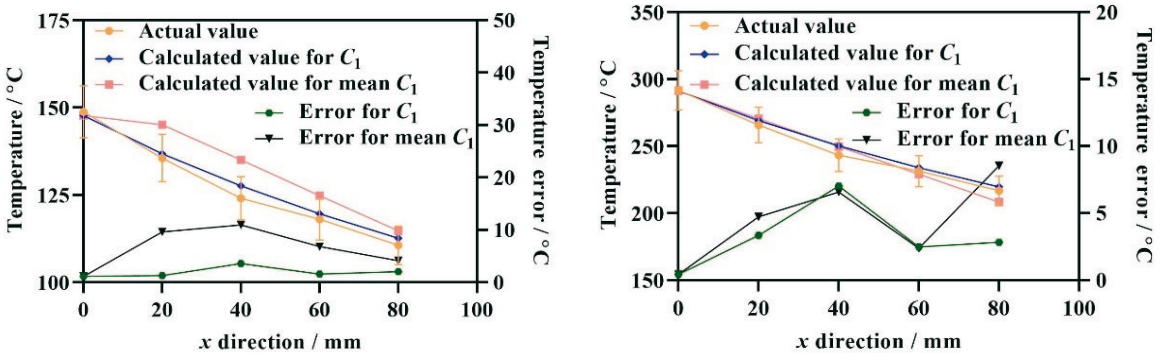

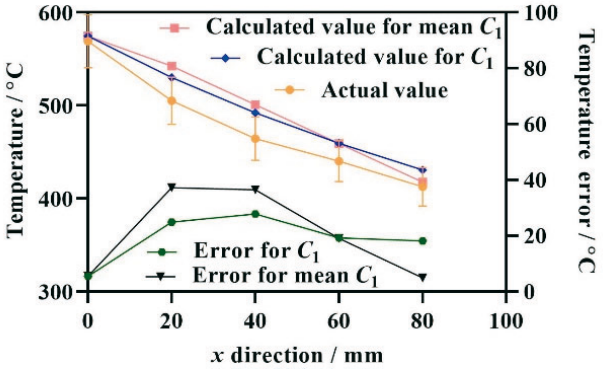

c)

Fig. 12 Error analysis of mean C_1 for each power: a) 50 W; b) 100 W, and c) 200 W

4. Conclusions

In order to rapidly forecast the temperature gradient of the forming region, a novel temperature calculated model is proposed to obtain the temperature distribution of the forming region during the preheating stage of belt heating in incremental sheet forming. The main conclusions of this study are given below:

1. The key calculated parameters of the model proposed is obtained through thermal transfer simulation, and the calculated accuracy of the model is less than 10% through corresponding physical experiments.
2. The heating transfer of the heating tube has a certain amount of heat loss in the preheating stage of belt heating in incremental sheet forming, and a heat loss rate of 4.5% is obtained to improve the calculated accuracy of the model.
3. The slope (C_1) of the calculated model changes with x and t, and the value of C_1 is mainly determined through x when t is constant. In addition, the mean value of C_1 can be used to simplify the calculated model of the temperature gradient when the calculated accuracy of the model is less than 10%.

Acknowledgement

This work was supported by the National Natural Science Foundation of China (grant No. 52205374 and 22272013), and the Special Basic Cooperative Research Programs of Yunnan Provincial Undergraduate Universities' Association (grant No. 202101BA070001-260), and the Scientific and Technological Research Program of Chongqing Science and Technology Bureau (grant No. cstc2021jcyj-msxm2910).

REFERENCES

[1] Wu R, Hu Q, Li M, Cai S, Chen S. Evaluation of the forming limit of incremental sheet forming based on ductile damage, Journal of Materials Processing Technology **2021**, 287, 1-8. https://doi.org/10.1016/j.jmatprotec.2019.116497

[2] Allwood J.M.; Braun D.; Music O. The effect of partially cut-out blanks on geometric accuracy in incremental sheet forming, Journal of Materials Processing Technology **2010**, 210(11), 1501-1510. https://doi.org/10.1016/j.jmatprotec.2010.04.008

[3] Gökhan Küçüktürk; Hilal Akıllılar. Investigating the Effect of Electron Beam Melting Parameters on the Ti6Al4V Alloy: A Simulation Study, Transactions of FAMENA 2022, 46(4), 45-58. https://doi.org/10.21278/TOF.464038121

[4] Hongwei Gao; Qinhong Fan; Zhibing Chu. Simulation Research on the Forming Process of Large Axles Rolled by Cross-Wedge Rolling, Transactions of FAMENA 2022, 46(3), 63-80. https://doi.org/10.21278/TOF.463043422

[5] Gökhan Küçüktürk; Mehmet Tahta; Hakan Gürün; Ibrahim Karaağaç. Evaluation of the Effects of Local Heating on Springback Behaviour for AHSS Docol 1400 Sheet Metal, Transactions of FAMENA 2022, 46(3), 51-62. https://doi.org/10.21278/TOF.463037821

[6] R. Matsumoto; Harutaka Sakaguchi; M. Otsu; H. Utsunomiya. Plastic joining of open-cell nickel foam and polymethyl methacrylate (PMMA) sheet by friction stir incremental forming, Journal of Materials Processing Technology **2020**, 282, 1-10. https://doi.org/10.1016/j.jmatprotec.2020.116691

[7] Dongwei Ao; Jun Gao; X. Chu; Shuxia Lin; Jun Lin. Formability and deformation mechanism of Ti-6Al-4V sheet under electropulsing assisted incremental forming, International Journal of Solids and Structures **2020**, 202, 357-367. https://doi.org/10.1016/j.ijsolstr.2020.06.028

[8] B. Saidi; Laurence Giraud Moreau; A. Cherouat; R. Nasri. Experimental and numerical study on warm single-point incremental sheet forming (WSPIF) of titanium alloy Ti-6Al-4V, using cartridge heaters, Journal of The Brazilian Society of Mechanical Sciences and Engineering **2020**, 43(10), 1-15. https://doi.org/10.1007/s40430-020-02632-8

[9] Chang Xu; Yanle Li; Zijian Wang; Zinan Cheng; Fuyuan Liu. The influence of self-lubricating coating during incremental sheet forming of TA1 sheet, International Journal of Advanced Manufacturing Technology **2020**, 110(9-10), 2465-2477. https://doi.org/10.1007/s00170-020-06013-2

[10] Mohanraj R.; Elangovan S. Thermal modeling and experimental investigation on the influences of the process parameters on warm incremental sheet metal forming of titanium grade 2 using electric heating technique, International Journal of Advanced Manufacturing Technology **2020**, 110(1-2), 255-274. https://doi.org/10.1007/s00170-020-05851-4

[11] Renhao Wu; Meng Li; Xinmei Liu; S. Cai; Jun Chen. Characterization of material flow in friction stir-assisted incremental forming with synchronous bonding of dissimilar sheet metals, International Journal of Advanced Manufacturing Technology **2020**, 109(9-12), 2523-2534. https://doi.org/10.1007/s00170-020-05782-0

[12] Duflou JR; Callebaut B; Verbert J; De Baerdemaeker H. Laser assisted incremental forming: formability and accuracy improvement, Cirp Annals-manufacturing Technology **2007**, 56(1), 273-276. https://doi.org/10.1016/j.cirp.2007.05.063

[13] Duflou JR; Callebaut B; Verbert J; De Baerdemaeker H. Improved SPIF performance through dynamic local heating, International Journal of Machine Tools & Manufacture **2008**, 48(5), 543-549. https://doi.org/10.1016/j.ijmachtools.2007.08.010

[14] Mohammadi A; Vanhove H; Van Bael A; Duflou JR. Towards accuracy improvement in single point incremental forming of shallow parts formed under laser assisted conditions, International Journal of Material Forming **2016**, 9(3), 339-351. https://doi.org/10.1007/s12289-014-1203-x

[15] Ji YH; Park JJ. Formability of magnesium AZ31 sheet in the incremental forming at warm temperature, Journal of Materials Processing Technology **2008**, 201(1), 354-358. https://doi.org/10.1016/j.jmatprotec.2007.11.206

[16] Galdos L; Argandona ESD; Ulacia I; Arruebarrena G. Warm incremental forming of magnesium alloys using hot fluid as heating media, Key Engineering Materials **2012**, 504-506, 815-820. https://doi.org/10.4028/www.scientific.net/KEM.504-506.815

[17] Fan G; Gao L; Hussain G; Wu Z. Electric hot incremental forming: a novel technique, International Journal of Machine Tools & Manufacture **2008**, 48(15), 1688-1692. https://doi.org/10.1016/j.ijmachtools.2008.07.010

[18] Fan G; Gao L. Mechanical property of Ti-6Al-4V sheet in one-sided electric hot incremental forming, International Journal of Advanced Manufacturing Technology **2014**, 72(5), 989-994. https://doi.org/10.1007/s00170-014-5733-7

[19] Al-Obaidi A; Kräusel V; Landgrebe D. Induction heating validation of dieless single-point incremental forming of AHSS, Journal of Materials Processing Technology **2017**, 1(1), 1-10. https://doi.org/10.3390/jmmp1010005

[20] Li Z; Lu S; Zhang T; Zhang C; Mao Z. 1060 Al electric hot incremental sheet forming process: analysis of dimensional accuracy and temperature, Transactions of the Indian Institute of Metals **2017**, 71(4), 961-970. https://doi.org/10.1007/s12666-017-1229-0

[21] Li Z; Lu S; Zhang T; Zhang C; Mao Z. Electric assistance hot incremental sheet forming: an integral heating design, International Journal of Advanced Manufacturing Technology **2018**, 96(9-12), 3209-3215. https://doi.org/10.1007/s00170-018-1792-5

[22] Pacheco PAP; Silveira ME. Numerical simulation of electric hot incremental sheet forming of 1050 aluminum with and without preheating, International Journal of Advanced Manufacturing Technology **2017**, 94(9-12), 3097-3108. https://doi.org/10.1007/s00170-017-0879-8

[23] Meier H; Magnus C; Buff B; Zhu J. Tool concepts and materials for incremental sheet metal forming with direct resistance heating, Key Engineering Materials **2013**, 549, 61-67. https://doi.org/10.4028/www.scientific.net/KEM.549.61

[24] Z. Li; B. Wu; Y. Sun; M. Shen; Z. Gao; Z. An; S. Lu. Improvement of arc burn defect of initial contact loss of electric hot incremental sheet forming, Mechanics & Industry **2022**, 23(11), 1-8. https://doi.org/10.1051/meca/2022012

Submitted: 17.4.2023

Accepted: 03.7.2023

Zhengfang Li
Yanping Sun
Bin Wu
Youwen Zhai
School of Mechanical and Electrical Engineering, Kunming University, Kunming 650214, China
Zhengyuan Gao*
Zhiguo An
School of Mechanotronics and Vehicle Engineering, Chongqing Jiaotong University, Chongqing 400074, China
*Corresponding author:
zhengyuangao@cqjtu.edu.cn